

Mitchell Thomas\* and Gilbert J. Friese\*\*  
L'Garde, Inc.  
Newport Beach, California

### Abstract

The low weight and packaged volume of inflatables relative to mechanical systems has long been known. A 700-meter diameter inflated reflector could be carried in a single shuttle payload. Surface tolerances were demonstrated resulting in acceptable gains for microwave wavelengths greater than 1 cm. The total system weight including replacement gas is comparable to or lower than mechanical systems for antenna diameters greater than 10-20 meters. The meteoroid problem is much less than originally anticipated because large antennas require only low inflation pressures. Mechanisms for antenna thermal control include optimized internal radiative exchange and the use of the pressurant as in a heat pipe.

### Nomenclature

|                   |   |
|-------------------|---|
| A                 | total area of holes in inflatable ( $\text{cm}^2$ )   |
| $A_0$             | meteoroid cross section ( $\text{cm}^2$ )   |
| $A_{\text{proj}}$ | space structure cross section in direction of meteoroids ( $\text{cm}^2$ )                                    |
| D                 | antenna maximum diameter (m or in)  |
| E                 | $2\varepsilon_i - \varepsilon_i^2$  |
| $E_G$             | product of film elastic modulus and thickness (lb/in)   |
| f                 | antenna focal length (m)  |
| F                 | incident solar flux divided by $\sigma$ , Stefan-Boltzmann constant ( $\text{K}^4$ )                          |
| g                 | meteoroid hole growth rate ( $\text{cm}^2 \text{sec}^{-1}$ )  |
| $\dot{h}$         | heat flux ( $\text{W cm}^{-2}$ )  |
| m                 | meteoroid mass (g)  |
| $m_i$             | inflatant mass (g, unless otherwise indicated in text)  |
| M                 | molecular weight (g)  |
| n                 | number of gores (flat segments) in antenna  |
| $n_i$             | molecular concentration ( $\text{cm}^{-3}$ )  |
| N                 | meteoroids of mass less than m impacting a sphere near the Earth's orbit ( $\text{cm}^{-2} \text{sec}^{-1}$ ) |
| $N_0$             | Avogadro number ( $6.025 \times 10^{23} \text{ mole}^{-1}$ )  |
| P                 | inflation pressure (psi)  |
| $P_{\text{para}}$ | paraboloidal antenna pressure (psi)   |
| $P_{\text{vap}}$  | vapor pressure (psi)  |
| $P_0$             | initial system inflation pressure (psi)   |
| r                 | meteoroid radius (cm)   |
| $r_t$             | torus small radius (m)  |
| R                 | radius of curvature (in)  |
| RG                | gas constant ( $8.32 \times 10^7 \text{ erg mole}^{-1} \text{K}^{-1}$ )                                       |
| $R_t$             | torus large radius (m)  |
| t                 | time (sec, unless otherwise indicated in text)  |
| $t_r$             | transmissivity  |
| T                 | temperature (K)   |
| $\bar{v}$         | mean molecular velocity ( $\text{cm sec}^{-1}$ )  |
| W                 | maximum gore width (in)   |
| $\alpha$          | solar absorptivity  |

|                 |   |
|-----------------|---|
| AH              | heat of vaporization ( $\text{cal g}^{-1}$ or $\text{J g}^{-1}$ ) |
| $\varepsilon_i$ | emissivity of inboard surface                                     |
| $\varepsilon_0$ | emissivity of outboard surface                                    |
| $\mu$           | Poisson's ratio   |
| $\rho$          | meteoroid density ( $\text{g cm}^{-3}$ )                          |
| $\rho_g$        | gas density ( $\text{g cm}^{-3}$ )                                |

### Concept of Pressurized Antenna

Large microwave space antennas that are shaped and maintained by gas pressure have many advantages. They can be fabricated and tested on the ground. They are not susceptible to launch vibrations and acoustics, and have excellent on-orbit dynamics. Large antennas can be placed into space without extravehicular activity. Typically, inflatables have a low cost for both development and production. Gas pressure attempts to perfect bodies of revolution, enhancing accuracy, in the presence of thermal distortions or manufacturing inaccuracies.

Sheldahl<sup>1</sup> contends for the fully inflated parabolic antenna, surface accuracies require no improvement for microwave performance, as demonstrated by tests on their 10-foot diameter inflatable demonstrator. Measured efficiencies of the 10-foot paraboloid were from 49.1 to 67.5% for frequencies from 2 to 4 GHz. The efficiency at 4 GHz should have been 80% due to measured surface RMS deviations of 3.4 mm; the measured data was close to this theoretical maximum, with the additional loss in gain experienced due to feed irregularities and scattering from feed and antenna supports.

Later, for the USAF ITV program and for NASA, L'Garde built 10-foot diameter inflated tori (Fig. 1), and measured surface flatness. The first torus had an rms surface accuracy of 1 mm and, with a slight correction to the tooling, the second had an accuracy of 0.77 mm (see Fig. 2). At 15 GHz the gain of a 0.77 mm accurate antenna would be 79% of the theoretical maximum.<sup>2</sup> Therefore, inflatables have been demonstrated to be clearly feasible for wavelengths longer than one centimeter, and have potential in the millimeter wave region.

The use of the fully inflated antenna can ease the problem of distortions caused by uneven thermal expansion. A recent report<sup>3</sup> rejected inflatable antenna concepts primarily because of the lack of thermal control. Actually, inflatables offer better thermal control opportunities than open structures. The radiative exchange between the sides of the inflatable can sharply reduce temperature non-uniformities. Special coatings on the Explorer IX balloon satellite<sup>4</sup> reduced the maximum AT across the balloon from 120°C to 30°C. The ability of these continuous area elements making up a balloon to control temperature caused NASA to seriously consider encapsulation of satellites in balloons as a method of thermal control.<sup>5</sup> Recently, Hughes

\*President, Associate Fellow AIAA

\*\*Program Manager

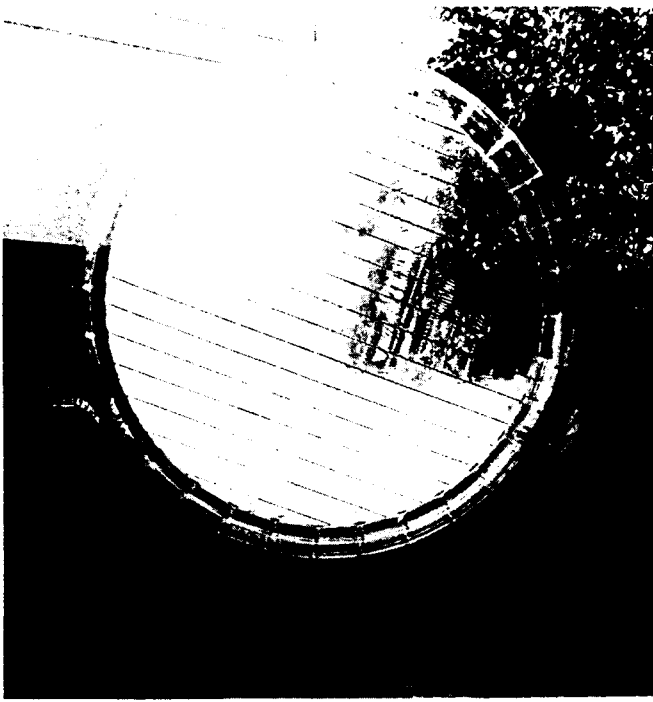


Fig 1 3-meter inflatable torus.

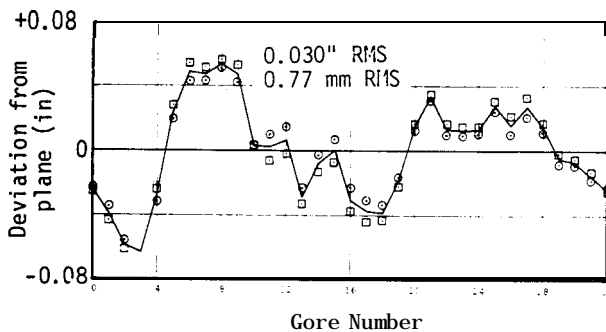


Fig. 2 Measured flatness of 3-meter diameter inflated torus.

has covered an antenna with a Kapton film solely to protect the antenna dish from temperature changes. In addition, a concept is described later to use the vapor from a surface-wetting liquid both to maintain inflation pressure, and to equilibrate temperatures through a heat-pipe-like effect. These thermal control mechanisms are not available to grid or open antennas.

One of the most significant advantages of the inflatable is its ability to fit in a small volume of nearly arbitrary shape. Furthermore, the weight of such devices appears competitive with the best mechanical concepts greater than 10 meters in diameter.

NASA has put considerable effort into making inflatable space structures, including Echo I and II, PAGEOS, and Explorer IX and XIX. Overall, inflatables in space have been successful, and the advantages mentioned above are real.

Continuous inflation for maintaining shape had not been seriously considered. Past research had focused on self-rigidizing inflatables, where

important advantages of inflatables diminish. Concern over meteoroid damage appears to have been and to be the major reason for discontinuing space inflatable work. However, this concern is not valid for large, low-pressure antennas. They can operate on the order of a decade with minimal replacement gas requirements. Figure 3 is an artist's concept of a parabolic pressurized antenna in orbit, with the maximum diameter held by an inflated and then rigidized torus (similar to the Echo II technique).

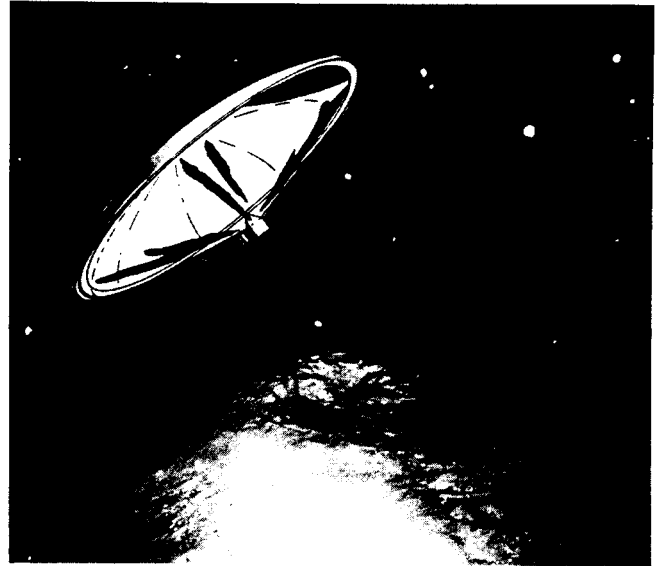


Fig. 3 Pressurized space antenna concept.

#### Antenna Pressurization Requirements

Gas leakage through seams or meteoroid holes directly influences the replacement-inflatable weight. Also, the antenna operating pressure directly affects this weight. The analysis below shows that the operating pressure of large antennas is sufficiently low so that they can operate in the meteoroid environment for many years. The replacement-inflatable weight is not excessive.

#### Meteoroids

Past analyses have tended to be conservative when considering meteoroid penetration of a space system, in order to assure system survival. More appropriate for the inflatable antenna, where the inflatable loss due to punctures will be replaced, is the use of the average anticipated flux of meteoroids. Our analysis to date has used the data of Whipple which includes satellite recorded data. In the following analysis these data were used and the following simplifying assumptions:

a. Hole size is given by the diameter of the "dirty snowball" low-density meteoroid ( $\rho = 0.1$ ).

b. A meteoroid penetrates only one surface. (Stony meteoroids would likely penetrate both sides of an inflated structure, but the hole size in this case would most likely be less than assumed.)

Theory for Hole Growth and Inflatable Requirements

The accumulated number of impacts per cm<sup>2</sup> per second is seen from reference 7 to be the following:

For log m < -5.2, N = 1.41(10)<sup>-14</sup> m<sup>-0.51</sup>, and

For log m > -5.2, N = 3.31(10)<sup>-19</sup> m<sup>-1.4</sup>

Similarly, the number of impacts per cm<sup>2</sup> per second with mass between m and m + dm is the following:

For log m < -5.2, dN = -7.19(10)<sup>-15</sup> m<sup>-1.51</sup> dm, and

For log m > -5.2, dN = -4.63(10)<sup>-19</sup> m<sup>-2.4</sup> dm

The change in meteoroid-produced hole area in time dt due to meteoroids of various sizes is given by dA = A<sub>proj</sub> ∫ A<sub>o</sub>(m) dN(m) dt. The individual hole area is given by the incident meteoroid cross section, namely A<sub>o</sub>(m) = πr<sup>2</sup>, where ρ  $\frac{4}{3}$  πr<sup>3</sup> = m.

Assuming that all incident meteoroids penetrate the surface, combination of the above relations and evaluation of the integrals leads to the following expression for the growth in meteoroid-produced hole area:

$$A(t)(\text{cm}^2\text{-sec}^{-1}) = A_{\text{proj}} 6.23(10)^{-14} t, t \text{ in secs (1)}$$

For comparison, the conservative value of hole growth used for PAGEOS analyses<sup>8</sup> was

$$A(t) = A_{\text{proj}} 1.11(10)^{-11} t \text{ (assuming } A_{\text{proj}} = \pi r^2, r = 3048 \text{ cm) (2)}$$

Also, the USAF near-Earth micrometeoroid environment is somewhat larger than that of Whipple. Other assumptions being the same, the USAF data<sup>9</sup> would predict a hole-growth rate about 2.5 times that of equation (1).

The PAGEOS satellite showed a transition from near spherocity to a more variable radius of curvature after about 22 days in orbit. Ref. 9 pointed out that this time corresponded to the predicted complete loss of pressurant based upon the upper estimate of equation (2). However, as pointed out in reference 10 (and a later section), there is a required optimum balloon pressure, deviation from which causes either billowing or flattening of balloon gores. An alternate explanation of the increase in fluctuation of apparent balloon radius of curvature reported<sup>8</sup> is that the pressure fell below that necessary to strain the gores into their proper shape and the film recovered partially toward its original flat state. This seems especially reasonable since the equation used to compute pressure loss in reference 8, namely equation (2), was an upper limit and not a probable case. The analysis below explores this hypothesis in more detail.

Using the elastic modulus for the PAGEOS balloon and the analysis of reference 10, [see equation (6) as given below], the optimum operating pressure for the balloon would be 0.045 torn PAGEOS was originally inflated to about 0.06 torr

by benzoic acid and relaxed down to 0.001 torr which was maintained by anthraquinone. The time to decrease below the optimum pressure is given by<sup>8</sup>

$$\ln\left(\frac{P}{P_0}\right) = 0.2877 = 5.423(10)^{-8} (3.325t + \frac{g}{2}t^2) \quad (3)$$

where g is the numerical coefficient in the area growth term -- equations (1) and (2). Using our value for g instead of the upper limit assumed in Ref. 9, the gores would begin to flatten per equation (3) after 333 hours. The observed transition at 22 days corresponds to 528 hours, which is not far from the above calculation, implying that the model we are using appears to be of the right order of magnitude.

The inflatable mass loss through the meteoroid holes can be computed from the free-molecular-flow kinetic relation dm<sub>i</sub> =  $\frac{1}{4}(n_i M/N_0) \bar{v} A(t) dt$  and  $\bar{v} = \sqrt{8R_G T/\pi M}$ . Using the perfect gas law, the mass loss can be computed by integrating the above equation, that is,

$$\Delta m_i (\text{lbs}) = 0.0119 \sqrt{M} P A_{\text{proj}} t^2, \quad (4)$$

for P in psi, A in cm<sup>2</sup> and t in years. This equation was used to help determine system weight as a function of lifetime. The operating pressure determination is presented later.

Weight and Package Volume

The weight of the pressurized antenna excluding electronics but including replacement inflatable is shown in Fig. 4 versus size and lifetime.

Data compiled by the Jet Propulsion Laboratory<sup>11</sup> for other advanced antennas are presented also. Pressurized antennas are relatively lightweight for diameters greater than 10 m. Similar data for packaged volume show the typical large advantage of inflatables as shown in Fig. 5.

If Fig. 4 is extrapolated to a space shuttle allowable payload weight of, say, 50,000 pounds, it is seen that a 700-meter diameter inflatable antenna could be carried. The antenna's package volume is 1000 cubic feet (Fig. 5 extrapolated) -- only about 10% of the shuttle's available volume.

Operating Pressure

The optimum pressure is a sphere or paraboloid (approximately) is<sup>10</sup>

$$P = \frac{4 \left[ \sqrt{2} \frac{n}{\pi} E_G \arcsin \left( \frac{\sin \pi/n}{\sqrt{5 + \cos^2(\pi/n)}} \right) - E_G \right]}{R (1 - \mu)}$$

For a large number of gores, n, equation 5 becomes

$$P = \frac{2W^2 E_G}{3(1 - \mu)RD^2} \quad (6)$$

Optimum pressure is that which strains each gore such that its centerline is equal in length to the seam (edge of the gore).

The optimum pressure is shown in Fig. 6 for a 1/2-mil thick Tedlar paraboloid. For the best

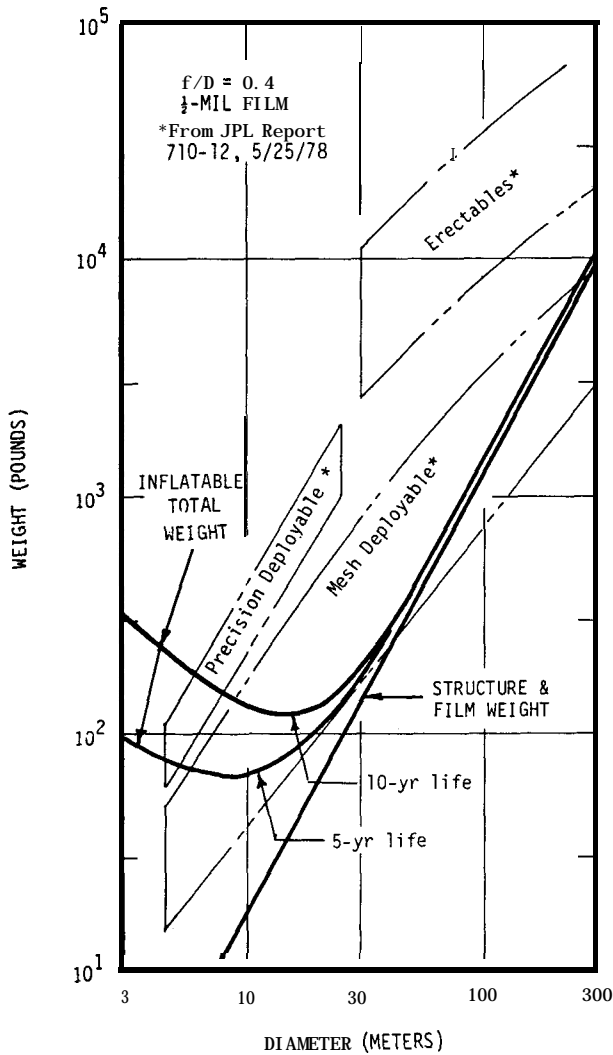


Fig. 4 Pressurized antenna system weight.

paraboloid shape, the antenna would be operated between the practical limits of 2" and 64" gore widths.

For an antenna  $f/D$  of 0.4, the radius of curvature  $R$  is approximately 0.86D. Then from equation (6), or the data from equation (5) in Fig. 6, the operating pressure scales like  $1/D$ . From equation (4) so does replacement inflatant mass. Therefore, as the antenna size increases, the replacement gas weight quickly becomes an insignificant portion of the overall weight.

A minimum pressure has not yet been established. It must be greater than the solar pressure of  $10^{-9}$  psi, and may be governed by attitude control forces and restoring time, or the gravity gradient.

For minimum weight, the antenna should be designed so that the optimum pressure equals the minimum required pressure. The optimum pressure of small antennas can be decreased somewhat by reducing the gore thickness and width, increasing the seam thickness, and/or using a low modulus material such as Teflon. The optimum pressure of large antennas (>500 meter dia) can be increased by doing just the opposite.

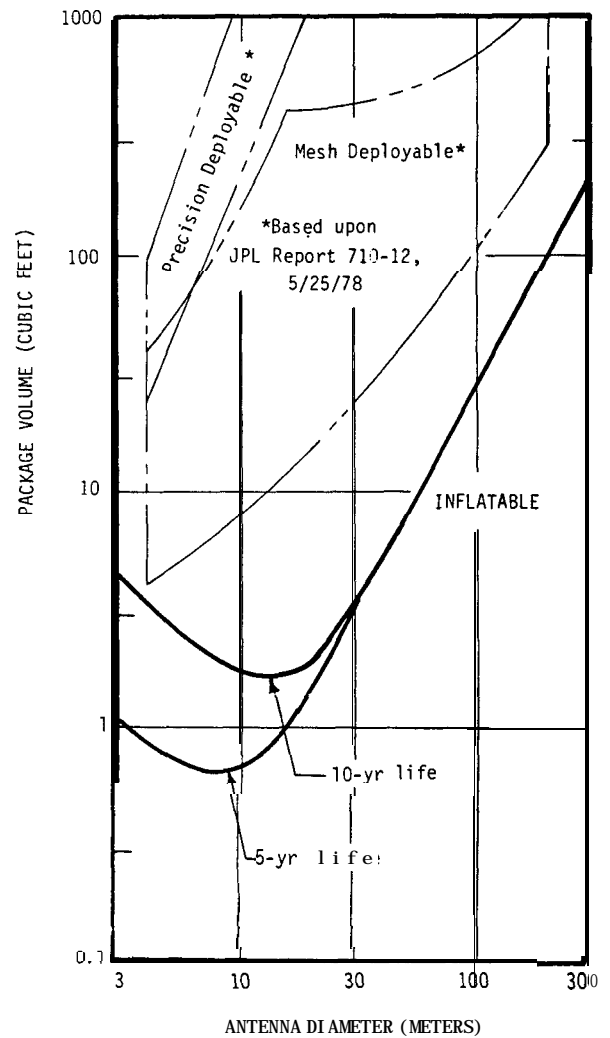


Fig. 5 Package volume for pressurized antenna.

While large inflatables operating at low pressure are practical for long time periods in space, the antenna rim (or torus) cannot be a simple inflatable. It can be shown that the pressure inside the torus must be

$$P_{\text{torus}} \geq (3R_t/4r_t)^2 P_{\text{para}} \quad (7)$$

where  $R_t$  and  $r_t$  are the torus large and small radii, respectively. For a 100-meter diameter antenna where  $P_{\text{para}} = 10^{-7}$  psi (Fig. 6), the torus pressure would have to be (for  $r_t = 1$  meter)  $1.4(10)^{-4}$  psi.

It would take about 7000 pounds of gas to maintain this pressure for ten years. With a self-rigidizing torus, the entire antenna system (including the pressure system) weighs only 1500 pounds (Fig. 4). Clearly, it is not practical to maintain such a torus inflated. Rigidizing techniques such as those qualified on the Echo II, Explorer IX and Explorer XIX satellites would be used for such a torus.

$$\epsilon_i^2 T_1^4 - (\epsilon_0^2 + \epsilon_0 E) T_2^4 = 0$$

Figure 7 shows solutions to these equations for the case  $\alpha/\epsilon_0 = 1$ . As seen by the data the temperature difference between the plates can be varied from 200°C to about 9°C for realistic values of the optical properties. This type of analysis can give general guidelines to the desired optical properties for the antenna film surfaces

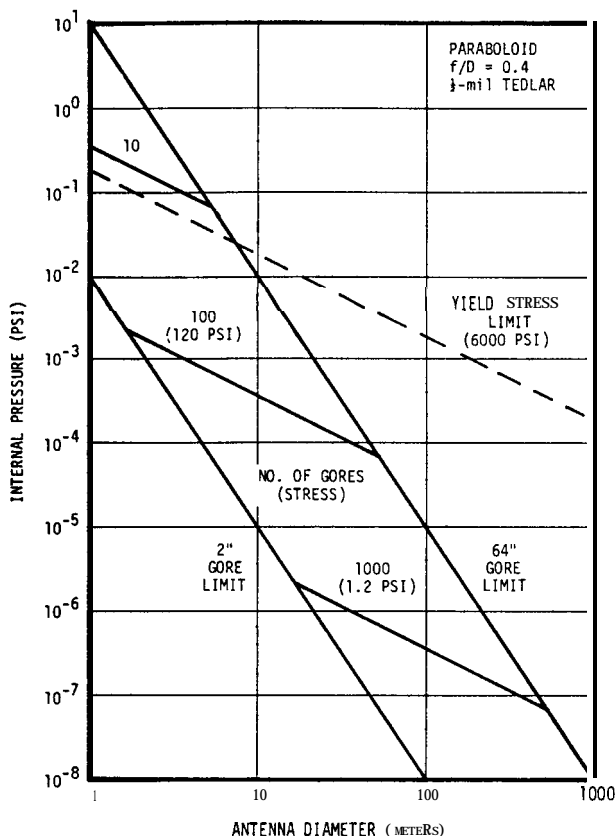


Fig. 6 Inflation pressure required for optimum shape.

### Thermal Distortions

Plastic films such as mylar or Kapton have coefficients of thermal expansion (CTE) of the order of  $10^{-5}/^{\circ}\text{F}$  while more stable composites, such as graphite epoxy have CTE's of the order of  $10^{-7}/^{\circ}\text{F}$ .<sup>12</sup> For large temperature differences on antennas in space, the thin film antennas would potentially distort 100 times more than the composite structures. This situation is not as bad as it might first seem, however. The type of distortion is different since inflatables tend to correct themselves while more rigid structures amplify any local distortion. Furthermore, mechanisms exist on inflatables to keep the maximum temperature differences to below  $10^{\circ}\text{C}$  whereas differences of  $200^{\circ}\text{C}$  would be expected on composite structures, between sunlit elements and those in the shade. Thus the net distortion of inflatables can be held to the same order of the best composite structures. Two techniques for keeping inflatable antennas isothermal are described below.

### Radiative Exchange

The magnitude of the maximum temperature difference between two infinite flat plates, one exposed to the sun, is given by the solution to the two equations

$$(\epsilon_i^2 + \epsilon_0 E) T_1^4 - \epsilon_i^2 T_2^4 = E F \alpha$$

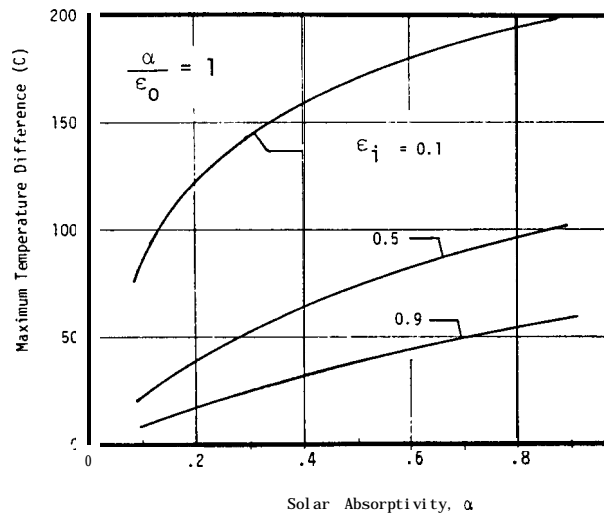


Fig. 7 Effect of radiative properties on temperature difference between parallel infinite plates.

For real plastic films, solar transmission is to be expected through the film for all but those that are metal coated. Fig. 8 shows data obtained by L'Garde for the transmission characteristics of standard white Tedlar and Melinex (polyester) films. Thinner films would be more transparent.

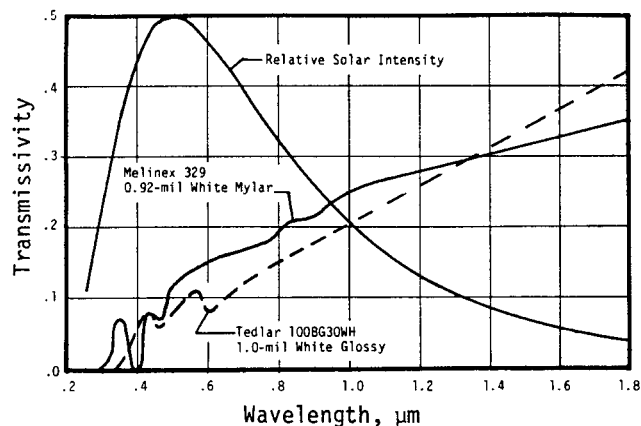


Fig. 8 Transparency of typical white films.

The effect of material transparency on the temperature distribution on a balloon structure is emphasized in the case of spherical balloons. The equilibrium temperatures of uniform, spherical, solar-absorbing, balloons exposed to the sun was calculated using an integral solution to the equation of transfer.<sup>13</sup> Internal reflections of sunlight were handled in a Monte Carlo analysis,

coupled to the integral solution. Temperature profiles are shown in Fig. 9. The large temperature fall off from the sunlit side is typical of high- $\alpha$  balloons (see Fig. 7). The effect of material transmission is also shown in Fig. 9. For semi-transparent materials, a hot spot appears on the "cold" side of the balloon due to the focusing effect of the sphere. This hot spot can be even hotter than the surface fully exposed to direct sunlight and exists for even very diffuse internal reflection characteristics. Although the radiative equilibrium solutions for the sunlit spherical balloon can be obtained in simple closed form for opaque balloons, numerical solutions are required for transmitting films.

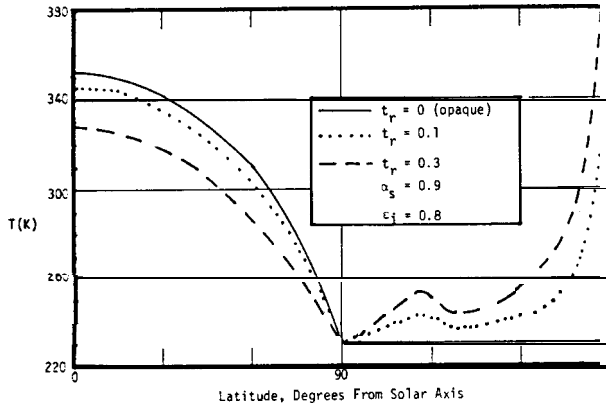


Fig. 9 Theoretical temperature profiles around semi-transparent spherical black balloons.

### Thermal Stabilization Using an Inflant

To our knowledge, no one has previously considered the use of an inflating gas both for system pressurization and also thermal control. The concept is to maintain system pressurization using a liquid with an appropriate vapor pressure. This liquid must also be attracted to the antenna wall so that the wall will be completely wetted, and it should have a large heat of vaporization. The concept is shown schematically in Fig. 10. A

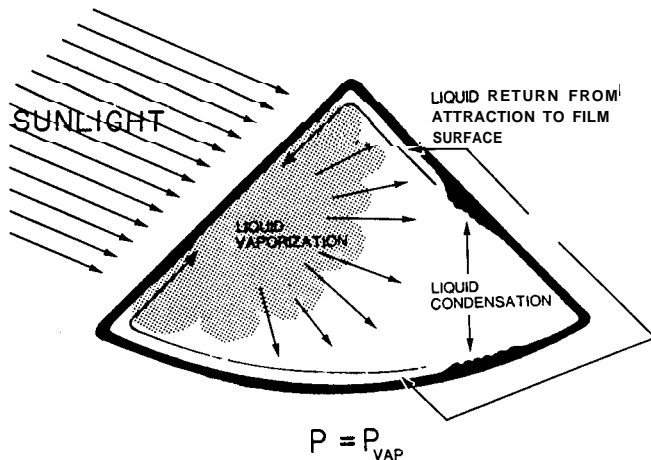


Fig. 10 Schematic of thermal control using inflant.

simple passive system for automatic pressure and temperature control results. The use of the heat-pipe-like effect of the inflating gas to maintain uniform antenna temperature is an inherent advantage of the inflatable antenna if it can be effectively exploited.

### Candidate Fluids

A variety of candidate liquids have been identified. The vapor pressure vs. temperature curves<sup>14</sup> for two of the more common materials, mercury and sulfuric acid, are shown in Fig. 11. Vapor pressures in the  $10^{-4}$  to  $10^{-7}$  psi range are available for system equilibrium temperatures of 325 to 250K -- easily obtainable with currently available optical coatings. These curves follow the usual Clapeyron-Clausius equation for phase change  $\log P = -\frac{A}{T} + B$  where A and B are constants.

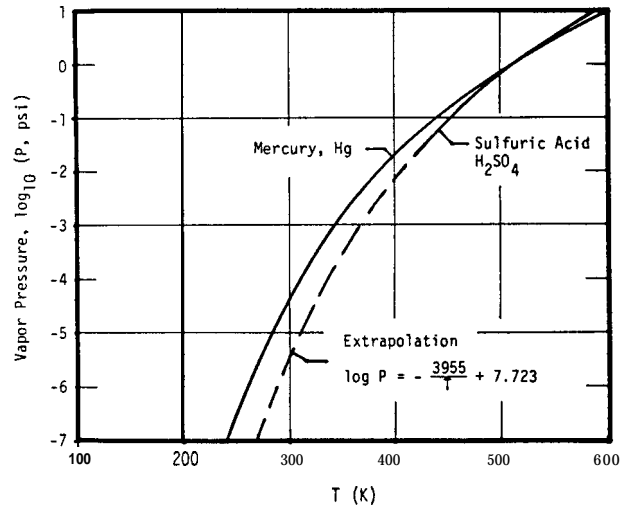


Fig. 11 Candidate liquid inflatants.

Other candidates are included in Table 1.

Table 1 Candidate liquid inflatants for thermal control.

| Name                | Formula                                       | M   | AH (cal/g) | Temperature for $P_{\text{vap}} = 1$ torr | Freezin Temp. |
|---------------------|---|-----|------------|---|---------------|
| Mercury             | Hg  | 80  | 65         | 357 c                                     | -39 c         |
| Sulfuric Acid       | H <sub>2</sub> SO <sub>4</sub>                | 98  | 122        | 330                                       | 10            |
| Formamide           | CH <sub>3</sub> NO                            | 45  | 346        | 70  | 3             |
| Glycerol            | C <sub>3</sub> H <sub>8</sub> O <sub>3</sub>  | 92  | 198        | 125                                       | 20            |
| 1, 2, 3 Butanetroil | C <sub>4</sub> H <sub>10</sub> O <sub>3</sub> | 106 | 154        | 102                                       | --            |
| Glutaric Acid       | C <sub>5</sub> H <sub>8</sub> O <sub>4</sub>  | 132 | 167        | 155                                       | 99            |

An interesting trade off concerns the steepness of the P vs. T curve, since the equilibrium temperature will vary with antenna/sun aspect. For a given allowable  $\Delta P$  in the antenna, there will be an associated allowable change in absorbed solar energy which can be related to the antenna f-number.

Another requirement of the liquid used is that it must wet the surface. Mercury is interesting in that it amalgamates with metals and may maintain

an aluminized surface at constant temperature. The ability of other liquids to wet the film surfaces is not presently known.

### Steady-State Temperature Model

A model is needed to define the heats of vaporization needed to maintain a near-uniform temperature across the antenna. For instance, the mass flux of atoms in a volume is given by

$\dot{m}_1 = \frac{1}{4} \rho_g \bar{v}$ . Using the usual definition of the mean molecular velocity,  $\bar{v}$ , and noting that each unit mass of gas is carrying energy away from the wall equal to the latent heat of vaporization,  $\Delta H$ , the total heat flux carried in the gas is

$$\dot{h} \text{ (w/cm}^2\text{)} = 0.011 \sqrt{MT} P \Delta H \text{ (P in psi)} \quad (8)$$

For mercury,  $\Delta H = 272 \text{ j/g}$ ; assuming a temperature of 250 K we have

$$\dot{h} = 427 P \text{ (w/cm}^2\text{)} \quad (9)$$

Assuming that about 10% of the incident solar flux is absorbed on one side of the antenna (typical for transparent or aluminized Kapton or mylar), the flux that need be carried internally is about

$0.013 \text{ w/cm}^2$ . This flux, from equation (9) can be carried by an internal pressure of  $3(10)^{-5} \text{ psi}$ . A more detailed model of the vaporization and heat transfer process is needed in order to determine the real restraints upon pressure and liquid heat of vaporization, depending upon incident heat load.

### Conclusion

Pressurized antennas have many advantages for space application when compared to mechanically-erected antennas. They can be kept continuously inflated for many years since the makeup inflatable requirements become a negligible part of system weight as the antenna gets bigger. For a 5 to 10 year lifetime, inflatable antennas are weight competitive for diameters greater than 10 or 20 meters. The low system weights result from the low inflation pressure required for large antennas.

With the use of high emissivities on the pressurized side of the antenna and low solar absorptivities on the exterior, internal radiative exchange can be used to minimize temperature differences across the antenna. Thermal distortions for such an antenna appear to be of the same order as distortions resulting when low CTE composite materials are used. Potentially, the inflatable used can act as a heat pipe which would essentially eliminate temperature gradients on the pressurized antenna. The pressurized antenna can be built with today's technology with large savings in cost over competing mechanical systems.

### Acknowledgements

The analysis presented and measurements of surface accuracy were supported entirely by L'Garde, Inc. The measurements of optical transmissivity of thin films were supported by Thiokol AstroMet. References for past efforts in inflatable space systems were provided by Robert James of NASA/Langley Research Center. Much of the work presented was stimulated by technical discussions with Robert Powell, Wolfgang Steuer, and Ewald Heer of the Jet

Propulsion Laboratory. An error in our earlier calculations of meteoroid penetration was pointed out to us by John Hedgepath of Astro Research.

### References

- <sup>1</sup> J. Wendt and L. D. Surber, "Unfurlable Antennas", Transactions of the Third Aerospace Expandable and Modular Structures Conference, AFAPL TR 68-17, May 16-18, 1967.
- <sup>2</sup> Microwave Performance Characterization of Large Space Antennas, Edited by D. A. Bathker, Report 77-21, Jet Propulsion Laboratory, May 15, 1977.
- <sup>3</sup> AAFE Large Deployable Antenna Development Program, NASA CR-2894, prepared by Harris Corporation, September 1979.
- <sup>4</sup> Claude W. Coffee, Jr., Walter E. Bressette, and Gerald M. Keating, Design of the NASA Lightweight Inflatable Satellites for the Determination of Atmospheric Density at Extreme Altitudes, NASA TN D-1243, April 1962.
- <sup>5</sup> George E. Sweet, An Experimental and Analytical Investigation of Balloon-Type Enclosures for Thermal Control of Satellites, NASA TN D-5230, June 1969.
- <sup>6</sup> Hughes News Release "Science/Scope", Aviation Week & Space Technology, February 18, 1980, p. 70.
- <sup>7</sup> Fred L. Whipple, "On Maintaining the Meteoritic Complex," presented at the Conference on Zodiacal Light and the Interplanetary Medium, Honolulu, Hawaii, January-February 1967.
- <sup>8</sup> Louis A. Teichman, The Fabrication and Testing of PAGEOS I, NASA TN D-4596, June 1968.
- <sup>9</sup> L. Jurich and T. L. Hoffman, "Concepts and Development of Expandable Manned Space Structures," Transactions of the Third Aerospace Expandable and Modular Structures Conference, AFAPL TR 68-17, May 16-18, 1967.
- <sup>10</sup> Investigation of a 15-KW Solar Dynamic Power System For Space Application, Contract AF-33(615)-7128, Sunstrand Aviation-Denver, Report Number AFAPL-TR-64-156, February 28, 1965.
- <sup>11</sup> R. E. Freeland, Industry Capability for Large Space Antenna Structures, Report 710-12, Jet Propulsion Laboratory, May 25, 1978.
- <sup>12</sup> A. A. Woods, Jr. "Offset Wrap Rib Concept and Development", Large Space Systems Technology - 1979, NASA Conference Publication 2118, 1980.
- <sup>13</sup> Tom J. Love, Radiative Heat Transfer, Charles E. Merrill Publishing Co., Columbus, Ohio, 1968.
- <sup>14</sup> Handbook of Chemistry and Physics, Chemical Rubber Publishing Co., 32nd Edition, 1950.